Deep Learning-Based Diagnostic Framework for Colorectal Cancer Using Histopathological Images

Ashif Al Nayem Zeesan

Electrical and Electronic Engineering
Islamic University of Technology
Dhaka, Bangladesh
ashifalnayem@iut-dhaka.edu

Md. Ahasanul Adib

Electrical and Electronic Engineering
Islamic University of Technology
Dhaka, Bangladesh
ahasanuladib@iut-dhaka.edu

Sadri Islam

Electrical and Electronic Engineering
Islamic University of Technology
Dhaka, Bangladesh
sadriislam@iut-dhaka.edu

Md. Touhidul Islam

Electrical and Electronic Engineering
Islamic University of Technology
Dhaka, Bangladesh
touhidulislam@iut-dhaka.edu

Abrar Fahim

Electrical and Electronic Engineering
Islamic University of Technology
Dhaka, Bangladesh
abrarfahim619@gmail.com

Fardin Sabahat Khan

Department of Accounting and MIS
University of Delaware
Delaware, USA
fardinsk@udel.edu

Abstract—Colon cancer is one of the most fatal cancers globally among both males and females, highlighting the urgent need for effective early detection methods to improve survival rates. Histopathological image analysis plays a critical role in identifying malignancy by examining cellular patterns, but traditional diagnostic methods can be time-consuming and resource-intensive, necessitating more efficient solutions. This study focuses on the colon-specific subset of the LC25000 dataset, a collection of high-resolution histopathological images, to develop a deep learning-based diagnostic framework using the MobileNetV2 architecture. A unique pre-processing technique including key steps like noise reduction, grayscale conversion, and dimensional standardization was employed to enhance image quality for model training. For colon cancer detection, the model achieved an overall accuracy of 99.95% with 100% recall, precision, and F1-scores. This architecture is designed to reduce computational power and processing time, which makes it highly suitable for mass utilization and resource-limited conditions. A comparative performance analysis was done with existing works to highlight the model's effectiveness in detecting colon cancer. These findings present the impact of the proposed work to develop a more reliable solution for colon cancer diagnosis.

Index Terms—Colon cancer, MobileNetV2, Histopathological images, Pre-processing, Image classification.

I. Introduction

Colon cancer has become increasingly common in both men and women, resulting from a combination of genetic tendencies and environmental factors. As per the World Health Organization, cancer is the leading cause of death globally with an estimated 28.4 million new cases projected by 2040 [1]. Additional cancer risk factors include lifestyle choices such as weight gain, physical inactivity, excessive alcohol intake, and poor eating patterns [2]. Age is a major, unavoidable risk factor for cancer, with 87% of cases emerging in individuals aged 50 and older [3]. A statistical study in the U.S. estimated that lung and colon cancers would rank among the three most common cancer types in 2020, with patients dealing with high death rates [4]. Cancer includes a wide

range of diseases, with colon cancer being one of the deadliest types, contributing around 10% of global cancer-related deaths [5]. Accurate diagnosis requires minimally invasive methods, as non-invasive methods alone can rarely perform precise characterization of tumors. The growth of colon cancer does not have a side effect at an early stage. The symptoms do not show till the disease makes significant progression.

Mitigating colon cancer death rates largely depends on early diagnosis and thorough screening. But accurate early detection remains difficult without diagnostic approaches such as tissue biopsies, CT scan and MRI. Regular screening is important for early detection in healthy individuals as well as patients already undergoing treatment. But constant testing also increases costs and places stress on medical workers. Computer-aided diagnostic systems are a powerful solution to minimize workload and error rates. These systems utilize deep learning (DL) architectures to examine large medical datasets more accurately and effectively and solve the challenges associated with the rapid increase of medical data.

The traditional method of screening cancer with histopathological images has been largely affected by technological advances like AI. This development enables quicker analysis and better decisions. Machine learning (ML) allows systems to learn specific tasks by processing data without requiring explicit programming [6]. ML algorithms are widely used in the biomedical sector to predict and classify various signals and images. In the same way, DL algorithms, that are meant to handle high dimensional data like multimodal anatomical images and videos contain artificial neural networks with multiple layers specially designed for classification tasks [7].

This work proposes a new DL-based study to identify colon cancer from histopathology images using the LC25000 dataset. This approach utilizes the MobileNetV2 transfer learning (TL) model, specifically designed to enhance diagnostic efficiency with less computational power.

II. LITERATURE REVIEW

Colorectal cancer can be classified as either colon cancer or rectal cancer, depending on where it develops. Early discovery remains difficult due to the overlapping cell structure, complicating diagnosis. In order to overcome this, current research has used artificial intelligence (AI) more and more to improve the accuracy and efficiency of cancer diagnosis utilizing histopathological images.

Shapcott et al. [8] presented a DL-based cell classification approach for colon cancer identification from histopathology images through region sampling focused on classification based on cell density, with features extracted through DL to ensure effective detection. Later, Garg et al. [9] applied a pre-trained Convolutional Neural Network (CNN) model for the prediction of lung and colon cancers. This work examined eight CNN-based models for classifying malignant and benign images, achieving promising accuracies.

Nur Ibrahim et al. [10] built a baseline CNN model for classifying four types of colon cancer. The study used histological images, with features extracted from 150 × 50 pixel textures. The model achieved an accuracy of 83%. Yildirim and Cinar [11] employed a specialized CNN model, MA_ColonNET, achieving an accuracy rate of 99.75% in classifying colon tissue types. This model, composed of 45 layers, demonstrated strong diagnostic reliability, helping to reduce diagnostic errors typically associated with manual evaluation methods. In a similar manner, Zarrin et al. [12] proposed a DL predictive model using MobileNetV2 and CNN-based layers, including Max and Average pooling. This study aimed to improve the classification of colon cancer images, achieving a peak accuracy of 99.67% with MobileNetV2.

M. Shahid et al. [13] utilised the AlexNet model in a modified form to classify colon and lung cancers using the LC25000 image dataset. Before training on the dataset, four layers of AlexNet were adjusted and the dataset images underwent various pre-processing steps. This optimized approach achieved an overall accuracy of 98.4%, proving to be computationally efficient for cancer detection. Mesut Toğaçar [14] introduced an AI-based approach to classify lung and colon cancer using the DarkNet-19 model for feature extraction, followed by Equilibrium and Manta Ray Foraging algorithm to eliminate low predictive value. The remaining features were classified with a Support Vector Machine (SVM), achieving an accuracy of 99.69%.

Following this, Chehade et al. [15] focused on different ML methods for the classification of lung and colon cancer subtypes by utilizing models like XGBoost, SVM, RF, LDA, MLP, and LightGBM. The study found XGBoost to be the top-performing classifier, with a peak accuracy of 99%. The study underscored the interpretability advantage of feature-engineered machine-learning models over deep learning, which functions more as a "black box" and is less interpretable. Al-Jabbar et al. [2] combined GoogLeNet, VGG-19, ANN, and PCA models to enhance the early

diagnosis of colon cancer, improving image quality through contrast adjustments and reducing high-dimensional data requirements. In parallel, Tummala et al. [1] employed the EfficientNetV2 model with Grad-CAM to create visual saliency maps that highlight key regions in histopathological images, aiding cancer subtype identification.

Hadiyoso et al. [16] utilized a VGG16-based CNN model with Contrast Limited Adaptive Histogram Equalization (CLAHE) to achieve consistent performance across various training epochs, while Singh et al. [17] introduced an ensemble method combining logistic regression, SVM, and random forest models, which yielded high accuracy but increased computational demands due to the ensemble structure. Khan et al. [18] proposed a model utilizing Vision Transformer (ViT) and a modified Swin Transformer for colon cancer detection. Using the LC25000 dataset, the Swin Transformer model achieved 99.80% accuracy, outperforming other models such as ResNet-101 and traditional ViT.

III. DATASET

In this study, the colon cancer subset from the Lung and Colon Cancer Histopathological Image Dataset (LC25000), published in 2020, was utilized [19]. The LC25000 dataset was collected at the James A. Haley Veterans' Hospital, Tampa, Florida, and is categorized, labeled, and augmented with rotations and flips by its authors. The LC25000 dataset contains 25,000 RGB histopathology images stained with hematoxylin and eosin of five classes of colon and lung tissues, 5,000 images of each class.

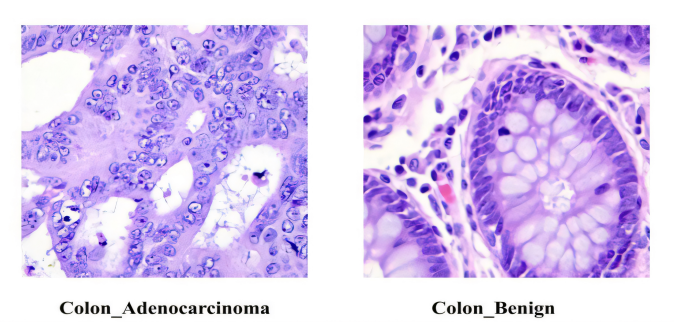


Fig. 1: Tissue Samples from LC25000 Datasets

Figure 1 depicts a sample of two classes from the colon cancer subset. The colon cancer subset includes 10,000 histopathological images divided into two classes: 5,000 images of colon Adenocarcinoma and 5,000 images of Benign colon tissue. All images are stained with hematoxylin and eosin, stored in JPEG format, and have a resolution of 768×768 pixels.

IV. METHODOLOGY

A. Overall Workflow

Figure 2 shows the entire framework of the proposed research. Firstly, the dataset is divided into training, testing, and validation subsets before pre-processing, with

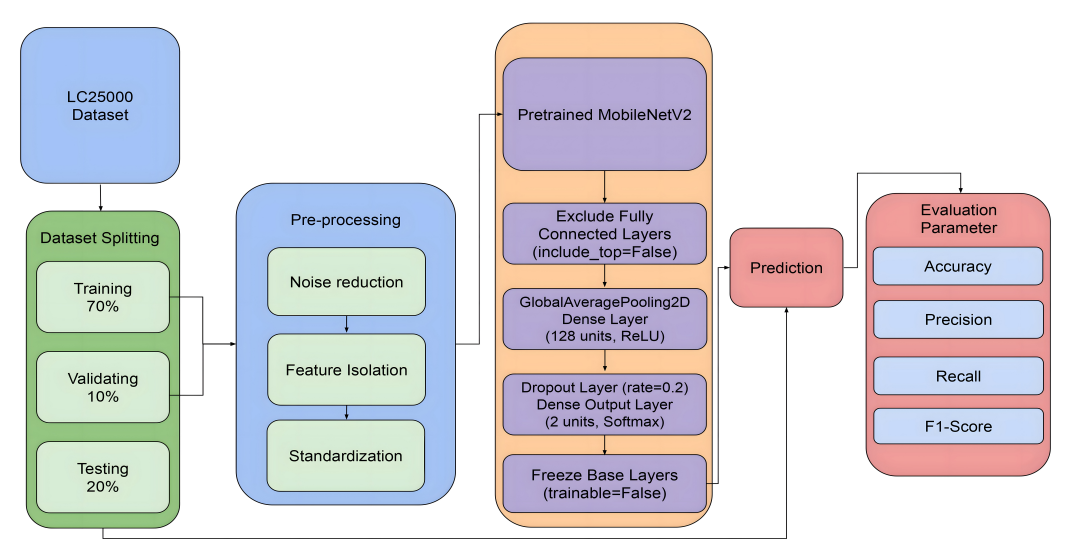


Fig. 2: Overall Workflow of the Study

a split ratio of 70:20:10. Then, the images from LC25000 dataset are transformed into grayscale format without losing important features. Furthermore, the improvements of contrast, brightness, and sharpness are applied to obtain better clarification. Noise reduction techniques like Gaussian blurring are used to remove artifacts while not losing sharpness at the edges. The binary thresholding routine is performed to highlight contours before cropping images according to extreme points.

The images are then resized to a standard resolution of 224x224 pixels. The MobileNetV2 architecture uses its pre-trained weights for feature extraction. This allows for precise classification of histopathological images into two categories. The workflow finishes with performance evaluation using metrics such as accuracy, precision, recall, and F1-score.

B. Train-Test Split

Initially, the dataset was split into a training set and a combined validation-test set. Thereafter, the combined validation-test set was further divided into separate validation and test sets. This process resulted in dividing the data into 70% for training, 20% for testing, and 10% for validation. Each image was mapped to its designated subset directory and transferred efficiently by using parallelization. Consequently, it provided a well-organized and balanced dataset, which is essential for reliable model training and evaluation.

C. Pre-processing

Figure 3 illustrates an overview of the entire pre-processing framework. Each image is converted in grayscale format, where the original workflow is applied to simplify the visual data while retaining essential features. The grayscale image is then transformed to PIL format for better enhancement. To enhance visual clarity, three key adjustments are performed: The contrast is amplified by a factor of 1.2 for greater disparity in tone, brightness is modified by 1.1 to uncover subtler details, and finally sharpness boosts the effective resolution via a value

of 1.2, creating a clearer picture. After such augmentations, the resulting images are in numpy array shape, which helps for the next steps on the pipeline.

Once enhanced, a Gaussian blur with a kernel size of (3, 3) is applied to minimize noise and smooth the image, which helps in isolating primary features. Following this, binary thresholding is conducted with a threshold value of 45 (on a 0–255 scale), binarizing the image and further reducing noise. This step is essential for contour detection, enabling the identification of distinct shapes within the image. If contours are detected, the algorithm determines the image's extreme points (top, bottom, left, and right) and crops the image accordingly, focusing on the most relevant area. If no contours are found, the image bypasses cropping and proceeds as-is to the following steps.

Noise reduction is further enhanced through bilateral filtering, which employs a diameter of 2 and sigma values of 50 for both color and spatial distances, effectively reducing noise without sacrificing edge sharpness. For enhanced visual differentiation, a pseudo-color transformation is applied using the bone color map, adding depth and contrast to the grayscale image. The processed image is then resized to a standardized 224x224 pixels, ensuring uniformity across the dataset. Finally, the image is saved, completing the overall pre-processing designed to optimize each image for model training.

D. MobileNetV2 Architecture

The proposed study uses the MobileNetV2 architecture, a DL model intended for transfer learning, and altered the architecture solely for the needs of colon image classification [20]. The architecture is designed to be efficient, producing high-quality images for classification tasks with less computing. The architecture uses depthwise separable convolutions that break down standard convolution operations into two smaller ones shown in figure 4. Then, the architecture reduces the parameters and operations on a lower

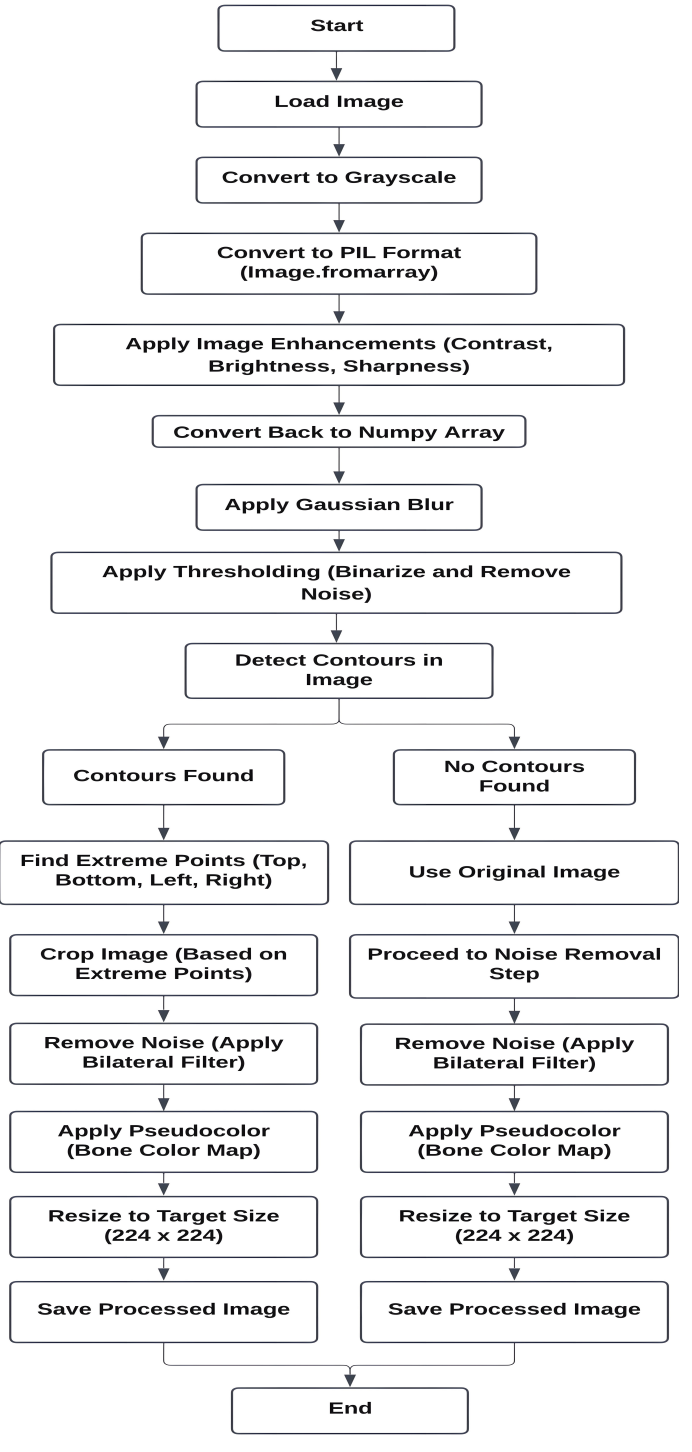


Fig. 3: Overall Pre-processing Framework

margin by selecting an optimal layout. It also uses inverted residual blocks with linear bottlenecks to capture the most important spatial features. So, the architecture can achieve higher accuracy with lower latency, proving its potential for constrained environments.

The top layer of the original pre-trained MobileNetV2 model (include_top=False) was removed. This change retains

the convolutional base, which acts as a feature extractor for the high-dimensional histopathological image data. Depthwise separable convolutions are a key building block for many efficient neural network architectures. Finally, the convolutional base uses depthwise separable convolutions and inverted residual blocks to provide efficient feature extraction while remaining computationally light.

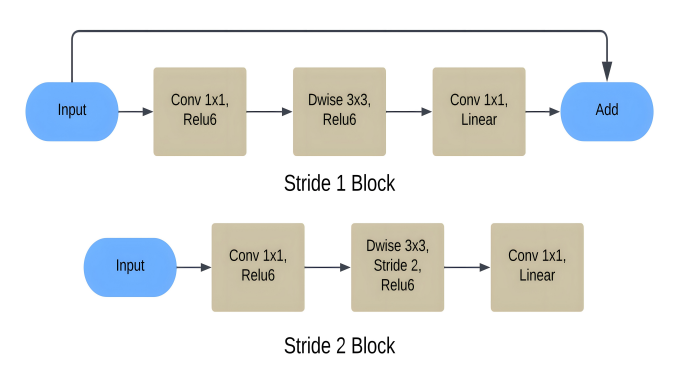


Fig. 4: MobileNetV2 Architecture(Residual and Inverted Residual Block)

Over the base pre-trained model, a sequence of custom layers was stacked in order to fine-tune the model for binary classification. Then a GlobalAveragePooling2D layer extracts the spatial features from the convolutional base while preserving essential information. Moreover, a Dense layer with 128 units and ReLU activation is deployed. A Dropout layer (rate = 0.2) regularizes the model and reduces overfitting. The architecture is frozen with a Dense output layer consisting of two units with softmax activation to allow accurate binary classification. The base layers of MobileNetV2 were kept static while training to preserve the pre-trained weights while only optimizing the newly added layers.

E. Performance Evaluation Metrics

The analysis used standard evaluation metrics, as outlined in Equations (1)–(4).

$$Accuracy = \frac{TP + TN}{TP + TN + FP + FN} \tag{1}$$

$$Precision = \frac{TP}{TP + FP}$$
 (2)

$$Recall = \frac{TP}{TP + FN} \tag{3}$$

F1 Score =
$$\frac{2 \times Precision \times Recall}{Precision + Recall}$$
 (4)

The True Positive (TP) recognizes normal data as normal, and True Negative(TN) stands for abnormal data, correctly classifying to its different classes of exceptionality. Both TP and TN are correct classifications. In contrast, if the data are abnormal but classified as normal, it is called False Positive (FP), while if they are normal and wrongly classified, this is called false negative (FN) [11].

V. RESULT ANALYSIS

The model was trained for 18 epochs. Table I presents information on training and validation loss and the accuracy for the last five epochs, during which the model achieved its highest training and validation accuracy. Figure 5 provides a comparative visualization of training and validation metrics, with one graph illustrating accuracy and the other depicting loss across all epochs.

TABLE I: Training and Validation Metrics for Last 5 Epochs

Epoch Number	Training Accuracy (%)	Training Loss (%)	Val. Accuracy (%)	Val. Loss (%)
14	99.77	0.51	100	0.0658
15	99.77	0.84	100	0.0216
16	99.75	0.73	100	0.0211
17	99.84	0.43	100	0.0417
18	99.91	0.25	100	0.0174

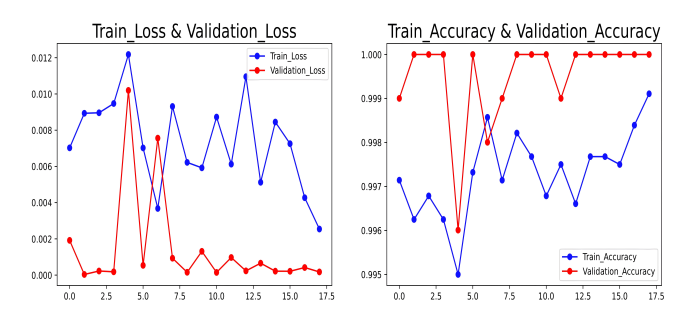


Fig. 5: Training and Validation Performance Comparison

Table II shows the performance of the model on the test set, which consists of data that were not used during the training phase. The evaluation metrics indicate exceptional performance across various aspects. It achieved a very low test loss of 0.1%, suggesting minimal error in predictions and strong alignment with actual values. With an overall accuracy of 99.95%, the model demonstrates high reliability in correctly classifying instances, indicating that nearly all predictions were accurate. The specificity at sensitivity metric, recorded at 1, signifies that the model attains perfect specificity when a predefined sensitivity threshold is maintained.

TABLE II: Test Set Model Evaluation Results

Overall	Test Loss	Test	Test AUC
Accuracy	(%)	Sensitivity	
(%)			
99.95	0.10	1	1

The confusion matrix displayed in figure 6 illustrates the model's performance on the test data. The matrix shows that the MobileNetV2 model achieves a high level of

accuracy across both categories, with only a single benign class image incorrectly identified as adenocarcinoma. This result highlights the model's reliability in detecting and distinguishing adenocarcinoma cancer cells from natural cells.

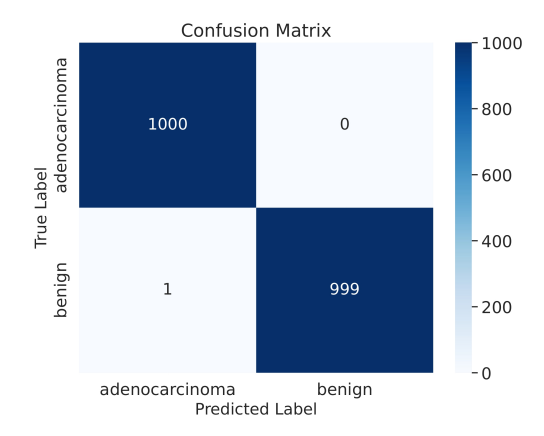


Fig. 6: Confusion Matrix for MobileNetV2

TABLE III: Classification Report Metrics

Class	Precision	Recall	F1-Score
	(%)	(%)	(%)
Adenocarcinoma	100	100	100
Benign	100	100	100

Table III provides the precision, recall, and F1-Score for the adenocarcinoma and benign classes. The model achieved 100% in all metrics for both classes. This result shows the model's accuracy in distinguishing the classes.

VI. COMPARATIVE ANALYSIS

Table IV shows a comparison among various existing architectures with the proposed work. Results show that MobileNetV2 achieved the highest accuracy of 99.95% and precision of 100%. Only the DCNN model was able to obtain the same precision score. This architecture outperformed models like MA_ColonNET, CoC-ResNet50V2, and XGBoost. The proposed work also shows a notable improvement over earlier models like ResNet50 and ResNet-v2. This demonstrates the impact of MobileNetV2's concise architecture for extracting relevant features.

VII. CONCLUSION

Early diagnosis of colon cancer is necessary to begin timely treatment and improve survival rates. This study presents a DL-based framework employing the MobileNetV2 architecture for detecting and classifying colon cancer from histopathological images. The proposed model achieved an excellent accuracy of 99.95%, addressing drawbacks in traditional methods. The model was trained on 7000 images and tested on 2000 images, where it correctly identified 1999 cases. These results show the model's potential for reliable and scalable colon cancer detection in clinical applications. In the future, the model can be adapted and tested on other types

TABLE IV: Comparisons with previous work.

Study\Paper	Architecture	Accuracy (%)	Precision (%)	Recall (%)
Bukhari et al. [21]	ResNet50	93.91	95.74	96.77
Gupta et al. [22]	ResNet-v2	90	96	87
Kishor et al. [23]	CoC-ResNet50V2	99.55	99.38	99.69
Chehade et al. [15]	XGBoost	99.3	99.5	99.5
Yildirim et al. [11]	MA_ColonNET	99.75	99.80	-
Hasan et al. [24]	DCNN	99.80	100	99.59
Proposed work	MobileNetV2	99.95	100	100

of cancer datasets to evaluate its performance in classification and prediction tasks.

VIII. CODE AVAILABILITY

The code will be shared upon request.

REFERENCES

- [1] S. Tummala, Seifedine Kadry, A. Nadeem, Hafiz Tayyab Rauf, and N. Gul, "An Explainable Classification Method Based on Complex Scaling in Histopathology Images for Lung and Colon Cancer," Diagnostics, vol. 13, no. 9, pp. 1594–1594, Apr. 2023, doi: https://doi.org/10.3390/diagnostics13091594.
- [2] M. Al-Jabbar, M. Alshahrani, E. M. Senan, and I. A. Ahmed, "Histopathological Analysis for Detecting Lung and Colon Cancer Malignancies Using Hybrid Systems with Fused Features," Bioengineering, vol. 10, no. 3, p. 383, Mar. 2023, doi: https://doi.org/10.3390/bioengineering10030383.
- [3] M. Sun, J. Wang, Q. Gong, and W. Huang, "Enhancing gland segmentation in colon histology images using an instance-aware diffusion model," Computers in Biology and Medicine, vol. 166, p. 107527, Sep. 2023, doi: https://doi.org/10.1016/j.compbiomed.2023.107527.
- [4] R. L. Siegel, K. D. Miller, and A. Jemal, "Cancer statistics, 2018," CA: A Cancer Journal for Clinicians, vol. 68, no. 1, pp. 7–30, Jan. 2018, doi: https://doi.org/10.3322/caac.21442.
- [5] M. Murugesan, R. Madonna Arieth, Shankarlal Balraj, and R. Nirmala, "Colon cancer stage detection in colonoscopy images using YOLOv3 MSF deep learning architecture," Biomedical Signal Processing and Control, vol. 80, pp. 104283–104283, Feb. 2023, doi: https://doi.org/10.1016/j.bspc.2022.104283.
- [6] D. Bazazeh and R. Shubair, "Comparative study of machine learning algorithms for breast cancer detection and diagnosis," 2016 5th International Conference on Electronic Devices, Systems and Applications (ICEDSA), Dec. 2016, doi: https://doi.org/10.1109/icedsa.2016.7818560.
- [7] J. Schmidhuber, "Deep learning in neural networks: An overview," Neural Networks, vol. 61, no. 61, pp. 85–117, Jan. 2015, doi: https://doi.org/10.1016/j.neunet.2014.09.003.
- [8] M. Shapcott, K. J. Hewitt, and N. Rajpoot, "Deep Learning With Sampling in Colon Cancer Histology," Frontiers in Bioengineering and Biotechnology, vol. 7, Mar. 2019, doi: https://doi.org/10.3389/fbioe.2019.00052.
- [9] S. Garg and S. Garg, "Prediction of lung and colon cancer through analysis of histopathological images by utilizing Pre-trained CNN models with visualization of class activation and saliency maps," 2020 3rd Artificial Intelligence and Cloud Computing Conference, Dec. 2020, doi: https://doi.org/10.1145/3442536.3442543.
- [10] N. Ibrahim, N. K. C. Pratiwi, M. A. Pramudito, and F. F. Taliningsih, "Non-Complex CNN Models for Colorectal Cancer (CRC) Classification Based on Histological Images," Lecture Notes in Electrical Engineering, pp. 509–516, 2021, doi: https://doi.org/10.1007/978-981-33-6926-9_44.
- [11] M. Yildirim and Ahmet Çinar, "Classification with respect to colon adenocarcinoma and colon benign tissue of colon histopathological images with a new CNN model: MA_ColonNET," International Journal of Imaging Systems and Technology, vol. 32, no. 1, pp. 155–162, Jul. 2021, doi: https://doi.org/10.1002/ima.22623.

- [12] Z. Tasnim et al., "Deep Learning Predictive Model for Colon Cancer Patient using CNN-based Classification," International Journal of Advanced Computer Science and Applications, vol. 12, no. 8, 2021, doi: https://doi.org/10.14569/ijacsa.2021.0120880.
- [13] S. Mehmood et al., "Malignancy Detection in Lung and Colon Histopathology Images Using Transfer Learning With Class Selective Image Processing," IEEE Access, vol. 10, pp. 25657–25668, 2022, doi: https://doi.org/10.1109/access.2022.3150924.
- [14] M. Toğaçar, "Disease type detection in lung and colon cancer images using the complement approach of inefficient sets," Computers in Biology and Medicine, vol. 137, p. 104827, Oct. 2021, doi: https://doi.org/10.1016/j.compbiomed.2021.104827.
- [15] Aya Hage Chehade, N. Abdallah, J.-M. Marion, Mohamad Oueidat, and P. Chauvet, "Lung and colon cancer classification using medical imaging: a feature engineering approach," vol. 45, no. 3, pp. 729–746, Jun. 2022, doi: https://doi.org/10.1007/s13246-022-01139-x.
- [16] Sugondo Hadiyoso, Suci Aulia, and Indrarini Dyah Irawati, "Diagnosis of lung and colon cancer based on clinical pathology images using convolutional neural network and CLAHE framework," International journal of applied science and engineering, vol. 20, no. 1, pp. 1–7, Jan. 2023, doi: https://doi.org/10.6703/ijase.202303_20(1).006.
- [17] O. Singh and Koushlendra Kumar Singh, "An approach to classify lung and colon cancer of histopathology images using deep feature extraction and an ensemble method," International Journal of Information Technology, vol. 15, no. 8, pp. 4149–4160, Sep. 2023, doi: https://doi.org/10.1007/s41870-023-01487-1.
- [18] KM. Arslan et al., "Migration Letters Classification Of Colon Cancer Using Deep Learning Techniques On Histopathological Images Migration Letters Classification Of Colon Cancer Using Deep Learning Techniques On Histopathological Images," vol. 21, no. S11, pp. 1741–8992, 2024.
- [19] A. A. Borkowski, M. M. Bui, L. B. Thomas, C. P. Wilson, L. A. DeLand, and S. M. Mastorides, "Lung and Colon Cancer Histopathological Image Dataset (LC25000)," arXiv:1912.12142 [cs, eess, q-bio], Dec. 2019, Available: https://arxiv.org/abs/1912.12142
- [20] M. Sandler, A. Howard, M. Zhu, A. Zhmoginov, and L.-C. Chen, "MobileNetV2: Inverted Residuals and Linear Bottlenecks," openaccess.thecvf.com, 2018.
- [21] S. U. K. Bukhari, A. Syed, S. K. A. Bokhari, S. S. Hussain, S. U. Armaghan, and S. S. H. Shah, "The Histological Diagnosis of Colonic Adenocarcinoma by Applying Partial Self Supervised Learning," Aug. 2020, doi: https://doi.org/10.1101/2020.08.15.20175760.
- [22] P. Gupta et al., "Colon Tissues Classification and Localization in Whole Slide Images Using Deep Learning," Diagnostics (Basel, Switzerland), vol. 11, no. 8, p. 1398, Aug. 2021, doi: https://doi.org/10.3390/diagnostics11081398.
- [23] Kishor R and Vinod Kumar R.S, "CoC-ResNet classification of colorectal cancer on histopathologic images using residual networks," Multimedia Tools and Applications, vol. 83, no. 19, pp. 56965–56989, Dec. 2023, doi: https://doi.org/10.1007/s11042-023-17740-5.
- [24] M. I. Hasan, M. S. Ali, M. H. Rahman, and M. K. Islam, "Automated Detection and Characterization of Colon Cancer with Deep Convolutional Neural Networks," Journal of Healthcare Engineering, vol. 2022, pp. 1–12, Aug. 2022, doi: https://doi.org/10.1155/2022/5269913.